JOURNAL OF BACTERIOLOGY, Apr. 2009, p. 2091–2101 Vol. 191, No. 7
0021-9193/09/$08.00+0 doi:10.1128/JB.00949-08

Differential Interactions between Tat-Specific Redox Enzyme Peptides and Their Chaperones▽†

Catherine S. Chan, Limei Chang, Kenton L. Rommens, and Raymond J. Turner*

Department of Biological Sciences, University of Calgary, Calgary, Alberta, Canada

Received 10 July 2008/Accepted 30 December 2008

The twin-arginine translocase (Tat) system is used by many bacteria to move proteins across the cytoplasmic membrane. Tat substrates are prefolded and contain a conserved SRRxFLK twin-arginine (RR) motif at their N termini. Many Tat substrates in *Escherichia coli* are cofactor-containing redox enzymes that have specific chaperones called redox enzyme maturation proteins (REMPs). Here we characterized the interactions between 10 REMPs and 15 RR peptides of known and predicted Tat-specific redox enzyme subunits. A combination of in vitro and in vivo experiments demonstrated that some REMPs were specific to a redox enzyme(s) of similar function, whereas others were less specific and bound peptides of unrelated enzymes. Results from Biacore surface plasmon resonance (SPR) and bacterial two-hybrid experiments identified interactions in addition to those found in far-Western experiments, suggesting that conformational freedom and/or other cellular factors may be required. Furthermore, we show that the interaction of the two prevents both from being proteolytically degraded in vivo, and kinetic data from SPR show up to 10-fold-tighter binding to the expected RR substrate when multiple binding partners existed. Investigations using full-length sequences of the RR proteins showed that the mature portion for some redox enzyme subunits is required for detection of the interactions. Sequence alignments among the REMPs and RR peptides indicated that homology between the REMPs and the hydrophobic regions following the RR motifs in the peptides correlates to cross-recognition.

The evolution of a diverse array of membrane-bound redox enzymes contributes to the ability of bacteria to grow in anoxic environments, using a variety of reductants or oxidants available for their electron transport chains. An example is in *Escherichia coli*, where a combination of 23 redox enzymes joined by the quinone pool work together, allowing *E. coli* to use a variety of electron acceptors under anaerobic conditions (reviewed in reference 23). These include dimethyl sulfoxide (DMSO), trimethylamine-*N*-oxide (TMAO), formate, nitrate, and others. Some redox enzymes are anchored at the cytoplasmic side of the membrane, but the majority of them are located at the periplasmic side. They also contain cofactors such as molybdopterin, Fe-S, and Ni-Fe clusters that are incorporated into the protein prior to their targeting and translocation across the cytoplasmic membrane.

Upon initial analysis, the operons encoding many redox enzymes appeared to contain an extra gene product that did not appear to be part of the final holoenzyme. After extensive investigation, these genes were found to encode chaperone proteins specific to the redox enzymes in that operon with apparent roles in the activation or assembly of the holoenzyme complexes. Given their unique and essential functions, our group previously reviewed the roles of such proteins and gave them the collective term of redox enzyme maturation protein (REMP), where a protein is defined as such when it is involved in the assembly of a complex redox enzyme but does not constitute part of the final holoenzyme (11, 29). The REMPs were further grouped into distinct families based on phylogenetic relationships (29).

The bacterial twin-arginine translocation (Tat) system was identified as the translocon for exporting bacterial redox enzymes in their folded and cofactor-containing forms. Primary sequence analysis showed that Tat substrates, including those which are not redox enzymes, contain a distinct SRRxFLK twin-arginine (RR) motif in their N-terminal sequences. This RR motif appears to always be located between the n and h regions of the tripartite signal (2). The translocating pore itself is comprised of three integral membrane proteins, TatA, TatB, and TatC, and a current model and mechanism of translocation is discussed and compared to the Sec system in a detailed review by Natale et al. (19).

Previous studies have shown that the REMPs DmsD and TorD interact with the RR-containing leader peptides of the catalytic subunits of DMSO and TMAO reductase, DmsA and TorA, respectively (20, 21). Furthermore, DmsD was shown to bind the preprotein form of TorA (20), yet this binding event was not observed for TorD and DmsA (12). In this study, we investigated whether specific or cross-interactions occurred between all predicted or known redox enzyme N-terminal/leader RR peptides and their REMPs listed in Table 1. The interactions identified from a combination of in vitro and in vivo methods demonstrate specificity of binding for some REMPs and a dependence on peptide display by the fusion tag. Quantitative comparisons of the dissociation constants for the interactions show that the REMPs bound their predicted substrate more tightly. Sequence alignments among the REMPs and RR peptides demonstrate that common interactions correlate to homology between the REMPs and the RR peptides, and experiments using the full-length RR

* Corresponding author. Mailing address: Department of Biological Sciences, BI 156 Biological Sciences Bldg., University of Calgary, 2500 University Dr., N.W., Calgary, Alberta, Canada T2N 1N4. Phone: (403) 220-3581. Fax: (403) 220-9311. E-mail: turnerr@ucalgary.ca.

† Supplemental material for this article may be found at http://jb.asm.org/.

▽ Published ahead of print on 16 January 2009.

TABLE 1. Tat-dependent redox enzyme systems targeted in this study[a]

Redox enzyme	RR-containing subunit(s)	Predicted REMP(s)	Catalytic cofactor
Biotin sulfoxide reductase 1	BisC	YcdY[b]	MoPt
Biotin/TMAO reductase	BisZ/TorZ	YcdY/TorD[b]	MoPt
TMAO reductase	TorA	TorD	MoPt
DMSO reductase	DmsA	DmsD	MoPt
Putative DMSO reductase	YnfE	DmsD[b]	MoPt[d]
Putative DMSO reductase	YnfF	DmsD[b]	MoPt[d]
DMSO/TMAO reductase	YedY	DmsD/TorD	MoPt[d]
Formate dehydrogenase	FdnG	FdhD/FdhE	MoPt
Formate dehydrogenase	FdoG	FdhD/FdhE	MoPt
Hydrogenase 1	HyaA	HyaE	Ni
Hydrogenase 2	HybO	HybE	Ni
Nitrate reductase (periplasmic)	NapA	NapD	MoPt
Nitrate reductase (cytoplasmic)	NarG	NarJ	MoPt
Nitrate reductase (cytoplasmic)	NarZ	NarW[b]	MoPt
Hypothetical protein	YfhG	?[c]	None predicted

[a] The predicted or known REMP(s) for each of the redox enzymes was investigated for interaction with peptides of the RR-containing subunits.
[b] Predicted REMP based on the predicted function/role of the enzyme and its relatedness to other enzymes with an appropriate REMP.
[c] No predicted REMP due to limited knowledge of the function of the enzyme.
[d] Predicted catalytic cofactor of MoPt based on the presence of a MoPt domain in its sequence.

proteins reveal additional clues for interactions from the mature region.

MATERIALS AND METHODS

Plasmid construction and growth conditions for far-Western studies. The *E. coli* REMPs NapD, NarJ, NarW, TorD, and YcdY were constructed with an N-terminal His_6-T_7 fusion as described previously for DmsD (20), using the primers listed in Table S1 in the supplemental material, into pRSET(A) (Invitrogen). FdhD, FdhE, HyaE, and HybE were generated similarly with the exception that a BamHI site instead of BclI was used. *E. coli* C41(DE3) (18) cells were transformed by the resulting plasmids (see Table S1 in the supplemental material) via heat shock (9), and plasmids isolated from ampicillin-resistant colonies were verified by sequencing.

Each RR peptide was constructed with a streptavidin-binding peptide and solubility enhancement tag 1 (SBP-SET1) fusion at its C terminus by cloning into pBEc-SBP-SET1 (Stratagene) as described previously (4), using the primers listed in Table S1 in the supplemental material. *E. coli* C41(DE3) cells were transformed and screened as described above. The TorA leader-glutathione *S*-transferase (GST) fusion was generated as described previously (20), and the TorA leader-green fluorescent protein (GFP) fusion was obtained from Santini et al. (25). The TorA leader-YFPc and RR peptide-YFPn fusions, corresponding to the C (residues 155 to 238) and N (residues 2 to 154) termini of yellow fluorescent protein (YFP) were generated similarly to the RR leader-T18 fusions described in "BACTH screening for interactions" below, using pIAF817YFP to generate host vectors containing the YFPn and YFPc fragments similarly to pUT18.

Cell cultures expressing the REMPs were grown in LB medium from a 1% (vol/vol) overnight subculture at 37°C until they reached an optical density at 600 nm of 0.4 to 0.6, at which point they were induced with 0.5 mM IPTG (isopropyl-β-D-thiogalactopyranoside) and then allowed to grow for another 3 h. Cultures were harvested by centrifugation at 2,700 × *g* and then resuspended in lysis buffer (50 mM Tris-HCl, 1 M NaCl, 1 mM dithiothreitol). Cell cultures expressing the RR peptides were grown as described above but were resuspended in Laemmli solubilization buffer (50 mM Tris-HCl [pH 6.8], 100 mM dithiothreitol, 5% [wt/vol] sodium dodecyl sulfate [SDS], 20% [vol/vol] glycerol, 0.1% [wt/vol] bromophenol blue).

Far-Western analysis of REMP and N-terminal/leader peptide binding. Each of the REMPs was purified as described previously (26). The average yields were ~10 mg/liter of culture, with yields ranging from 3 mg/liter to 22 mg/liter. The peptide-containing extracts were separated via 15% SDS-polyacrylamide gel electrophoresis (SDS-PAGE) and transferred to a nitrocellulose membrane as described previously (4). Membranes were then incubated in solutions containing 15, 40, 75, or 100 μg/ml of each of the purified REMPs and detected using 1:5,000 anti-T_7 Tag antibody (horseradish peroxidase [HRP] conjugated) (Novagen).

For the other peptide fusion constructs shown in Fig. 4A, cell extracts were separated by 12% SDS-PAGE and treated as described above but incubated with 100 μg/ml REMPs only. Western blotting to confirm expression of all peptide fusions was done with 100 or 350 ng/ml streptavidin-HRP (Pierce) against SBP, 1:500 anti-CyaA polyclonal antibody (Santa Cruz Biotechnology) against the T18 portion of adenylate cyclase, 1:4,000 anti-GST monoclonal antibody (Novagen) against GST, and 1:2,000 Living Colors full-length A.v. polyclonal antibody (Clontech) for GFP, YFPn, and YFPc.

Biacore SPR analysis of REMP/RR peptide interactions. Cytoplasmic fractions from cells harboring the N-terminal/leader plasmids (see Table S1 in the supplemental material) were grown, processed, and fractionated as described previously (4). Following dialysis to remove endogenous biotin, the cytosol was used directly for immobilization on sensor chips containing streptavidin (sensor chip SA; GE Healthcare) at 200 μg/ml of total protein; experiments were done with surface-bound RR peptide corresponding to ~300 to 500 resonance units. Experiments were carried out in running buffer containing 10 mM HEPES (pH 7.4), 150 mM NaCl, 50 μM EDTA, and 0.0005% vol/vol Surfactant P20 (GE Healthcare). Each of the REMPs was analyzed for binding by injecting 100 μl of a 200-μg/ml purified sample at a flow rate of 20 μl/min. REMPs showing an interaction at this concentration were subsequently tested at concentrations of 100, 75, 50, 25, 10, and 5 μg/ml. Three 1-minute pulses of 10× regeneration solution (1 M NaCl, 50 mM NaOH) were used to regenerate the chip after each injection. Kinetic data analysis for the pairs showing interactions was done with BIAevaluation software v. 4.0 for the multiple concentrations simultaneously using a 1:1 Langmiur model. Some data curves were eliminated to reduce the χ^2 value for a better fitting; all data sets had a χ^2 value of between 2 and 5.

Plasmid constructs for bacterial two-hybrid (BACTH) studies. Each REMP and RR peptide or RR protein was cloned with the T25 and T18 portions, respectively, of *Bordetella pertussis* adenylate cyclase at their C termini. An interaction between the REMP and RR peptide/protein brings the two fragments of adenylate cyclase together and restores cyclic AMP (cAMP) production in a *cya*-deficient strain containing a *mal* reporter (*E. coli* BTH101). To generate the fusions, PCR amplification using the primer pairs listed in Table S1 in the supplemental material added a HindIII or SphI site at the 5′ end and a KpnI or XbaI site at the 3′ end. The PCR products were digested with HindIII/SphI and KpnI/XbaI and cloned into pKNT25 and pUT18 (14). Following screening for ampicillin or kanamycin resistance on LB agar plates, plasmids isolated from the individual colonies were sequenced as described above.

BACTH screening for interactions. For the in vivo BACTH screening, *E. coli* BTH101 (15) competent cells were transformed by the REMP-T25 plasmids (see Table S1 in the supplemental material) and screened on LB agar plates containing kanamycin. New competent cells carrying the REMP plasmids were made from the positive clones and were then transformed by plasmids encoding RR peptide/protein-T18 (see Table S1 in the supplemental material) and screened on MacConkey agar plates containing kanamycin and ampicillin at 30°C for 3 days. For the red/white screening, the color of colonies from the individual REMP and RR peptide/protein pairs was observed after 3 days. For the liquid

A

```
                                  SRRxFLK
BisC   ---------------MANSSSRYSVLTAAHWGPMLVETDGETVFSSRGALATGMENSLQSAVRDQ-   50
BisZ   ---------------MT--LTRREFIKHSG-----IAAGAL-VVTSAAPL---P-----------   28
DmsA   ------MKTKIPDAVLAAEVSRRGLVKTT------AIGGLA-MASSALTLPFSRI----------   42
FdnG   ---------------MD--VSRRQFFK--------ICAGGM-AGTTVAALGFAPKQ----------   30
FdoG   ---------------MQ--VSRRQFFK--------ICAGGM-AGTTAAALGFAPSV----------   30
HyaA   ----MNNEETFYQAMRRQGVTRRSFLK---------YCSLA-ATSLGLGAGMAPKI----------   42
HybO   -------MTGDNTLIHSHGINRRDFMK---------LCAAL-AATMGLSSK---------------   34
NapA   ---------------MK--LSRRSFMKAN------AVAAAA-AAAG-LSVPGV-------------   28
NarG   ---------------MSKFLDRFRYFKQKGETFADGHGQLL-NTNRDWEDGYRQRWQHDKIVRSTH   50
NarZ   ---------------MSKLLDRFRYFKQKGETFADGHGQVM-HSNRDWEDSYRQRWQFDKIVRSTH   50
TorA   ---------MNNNDLFQ--ASRRFLA--------QLGGLT-VAGMLGPSLLTPRR----------   36
YedY   MKKNQFLKESDVTAESVFFMKRRQVLKALG-ISATALSLPHA-----------------------   41
YfhG   -----------MRHIFQRLLPRRLWLAGLP--CLALLGCVQNHNKPAIDTPAEEKIPV--------   45
YnfE   ------MSKN--ERMVG--ISRRTLVKST------AIGSLA-LAAGGFSLPFTLRN----------   39
YnfF   ------MKIHTTEALMKAEISRRSLMKTS------ALGSLA-LASSAFTLPFSQM----------   42
SufI   ---------------MSL--SRRQFIQASG------IALCAG-AVPLK------------------   24
OmpA   MKKTAIAIAVALAGFATV                                                  18
```

B

DmsD interactors

```
                    :*.*::*.  . :*  .
DmsA            TTAIGGLAMASS-ALTLPFSRI- 42
YnfF            TSALGSLALASS-AFTLPFSQM- 42
YnfE            STAIGSLALAAG-GFSLPFTLRN 39
TorA            --QLGGLTVAGMLGPSLLTPRR- 36
```

NapD interactors

```
                          ** **: ***
NapA            ANAVAAAAAAAGLSVPGV 28
HybO            --LCAALAATMGLSSK-  34
```

FdhE interactors

```
                **********.*******.
FdnG            ICAGGMAGTTVAALGFAPKQ 30
FdoG            ICAGGMAGTTAAALGFAPSV 30
```

NarJ/W interactors

```
                ************::::******.******.********
NarG            QKGETFADGHGQLLNTNRDWEDGYRQRWQHDKIVRSTH 50
NarZ            QKGETFADGHGQVMHSNRDWEDSYRQRWQFDKIVRSTH 50
```

FIG. 1. Sequence alignment of RR peptides. (A) Alignment of the full sequences of RR peptides used in this study. The two controls, OmpA and SufI, are included for comparison. The RR motif is highlighted in bold. (B) Alignment of the hydrophobic region immediately following the RR motif, based on RR peptides interacting with a common REMP. The continuous stretch of small hydrophobic residues that may play a role in recognition specificity by the REMPs is shaded. Residues in the alignment that are identical (*), conserved substitutions (:), and semiconserved substitutions (.) are indicated. Numbering is based on the original positions of residues in the full-length RR peptide. Both panels were generated using ClustalW (5).

culture assay, a minimum of three colonies per pair from the 3-day-old plates were picked and grown in LB medium containing ampicillin and kanamycin at 30°C overnight. The next morning, 1.5 ml of culture was harvested and washed in Z buffer, and a fixed-time enzymatic assay using 100 μl of washed cells was performed as described by Miller (17). The assay was done at 30°C for 30 min prior to quenching with sodium carbonate. Protein expression studies of the REMP and peptide fusions were done with 1 ml of overnight culture inoculated from the above-described plates, which was harvested and resuspended in 100 μl Laemmli solubilization buffer prior to SDS-PAGE and Western blotting as described above. The T25 and T18 adenylate cyclase portions were detected with anti-CyaA antibody described above.

RESULTS

In vitro far-Western analysis of interactions. The redox enzymes, their RR motif-containing subunit, and their predicted REMP targeted for investigation in this study are listed in Table 1. The leaders of OmpA, a Sec-dependent protein, and SufI, a Tat-dependent protein with no apparent REMP/chaperone, were also included in all of our studies to serve as negative controls. The amino acid sequence chosen for the N-terminal/leader RR peptides was based on the presence of a signal peptidase I cleavage site predicted by SignalP (1) and terminated prior to the cleavage sequence. For sequences appearing to lack a cleavage site, the residues were truncated after 50 amino acids. A multisequence alignment of the RR peptides used in this study generated using ClustalW (5) is shown in Fig. 1A. The alignment shows that the peptides of BisC, NarG, and NarZ differ most from the consensus SRRxFLK motif in that they all contain only one of the two arginine residues. They are cytoplasmically anchored enzymes

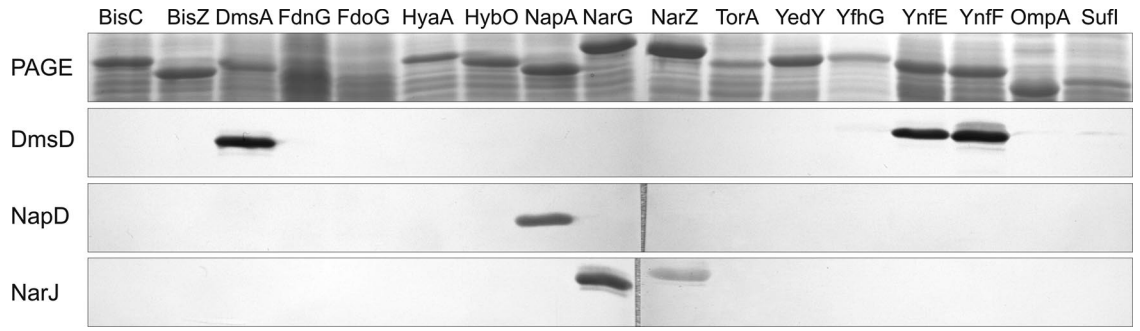

FIG. 2. Far-Western analysis of interactions. Approximately equal amounts of peptide extracts were separated by SDS-PAGE (PAGE row) and then blotted. Only REMPs showing an interaction are included. Blots were probed with 15, 40, 75, or 100 μg/ml of purified REMPs; blots with 100 μg/ml are shown.

and have been described to contain vestige or remnant Tat signal peptides that may have been inactivated over the course of evolution (27, 29).

Previous studies demonstrated the interaction of DmsD and NarJ with the DmsA leader and NarG N-terminal peptide, respectively, using a far-Western method (4, 26). Using a similar method, blots containing PAGE-separated cell extracts with overexpressed RR peptides fused to SBP were incubated with solutions of various concentrations of purified REMP. An interaction between the two results in the immobilization of the REMP, which is then detected via a tag-specific antibody to the REMPs. Utilizing this method, only DmsD, NapD, and NarJ showed interactions with the RR peptides (Fig. 2). DmsD bound the leader peptides of YnfE and YnfF in addition to DmsA; this was not surprising, as these two are homologues of DmsA at 43% and 56% sequence identity and 60% and 81% sequence similarity, respectively. NarJ bound NarG, its expected substrate, and NarZ of another cytoplasmic nitrate reductase. NapD was also shown to bind its expected substrate of the NapA leader. It should be noted that the peptides of FdnG and FdoG did not accumulate in the cell despite multiple induction and growth conditions as confirmed by probing with 350-ng/ml streptavidin-HRP, compared to the 100 ng/ml that was sufficient to detect all other RR peptide-SBP proteins on a Western blot (results not shown). Attempts using a different fusion partner (see below) resulted in accumulation of the two, but no interactions with any of the REMPs were detected either.

Since the blots were probed with four different concentrations of REMP solutions (15, 40, 75, or 100 μg/ml), a summary of the strengths of the interactions is shown in Table 2. As approximately equal amounts of the N-terminal/leader peptides were loaded onto the gels (Fig. 2, PAGE row), the observation of an interaction at the lowest concentration of REMP was used as an indication of the strength. For example, an interaction was observed between DmsD and DmsA leader at the lowest concentration of 15 μg/ml, and therefore its interaction is the strongest. An interaction between NarJ and NarZ peptide was observed only at the highest concentration of 100 μg/ml, indicating a weaker interaction. Western blots against the SBP tag could not be used as a comparison of the amounts present, as some peptides showed a far stronger antibody interaction even though the PAGE gel showed similar amounts of protein present (results not shown).

TABLE 2. Relative binding affinities of the REMPs DmsD, NapD, and NarJ

REMP	Affinity[a] with:					
	DmsA	NapA	NarG	NarZ	YnfE	YnfF
DmsD	++++				+++	++++
NapD		+++				
NarJ			++	+		

[a] Affinity levels are based on the minimum concentration of REMP required to obtain a signal on the far-Western blots. The highest-affinity binding (++++) is defined as a signal observed with the lowest concentration of REMP (15 μg/ml), and the lowest-affinity binding (+) is defined as that observed with the highest concentration of REMP (100 μg/ml).

The results using a dot blot far-Western where cell extracts are spotted onto a membrane directly and the proteins are not required to refold on the membrane showed results similar to those described above (not shown).

BACTH analysis of interactions. An in vivo BACTH assay (14, 15) was also used for screening of interactions. Two methods were used to screen for interactions between the REMPs and N-terminal/leader peptides: a red/white colony assay on MacConkey agar plates based on the *mal* reporter gene and a liquid culture assay based on the *lacZ* reporter gene. The red/white assay is based on the production of acidic products that turn the colony red when the *mal* reporter gene is turned on in the presence of cAMP. The liquid culture assay is based on the activation and production of β-galactosidase by cAMP, which is enzymatically assayed using the substrate *ortho*-nitrophenyl-β-galactoside. Based on observation of the colony color, an interaction was seen between the same REMPs and RR peptides as seen by the far-Western analysis, with the exception that an interaction was also observed for TorD with TorA leader and for NarJ with NarZ peptide, producing white colonies with a small red center (results not shown). When the liquid culture assay was performed, the results were the same as for the colony assay, except that an interaction between NapD and HybO leader peptide was also detected (Fig. 3A). This interaction, however, was not consistently observed and exhibited "all-or-nothing" levels of β-galactosidase activity. Additional testing revealed that the interaction between these two is time dependent, where colonies were taken once a week for the liquid assays from plates grown at 30°C for 3 days and then kept in 4°C for up to 40 days. During this testing it was

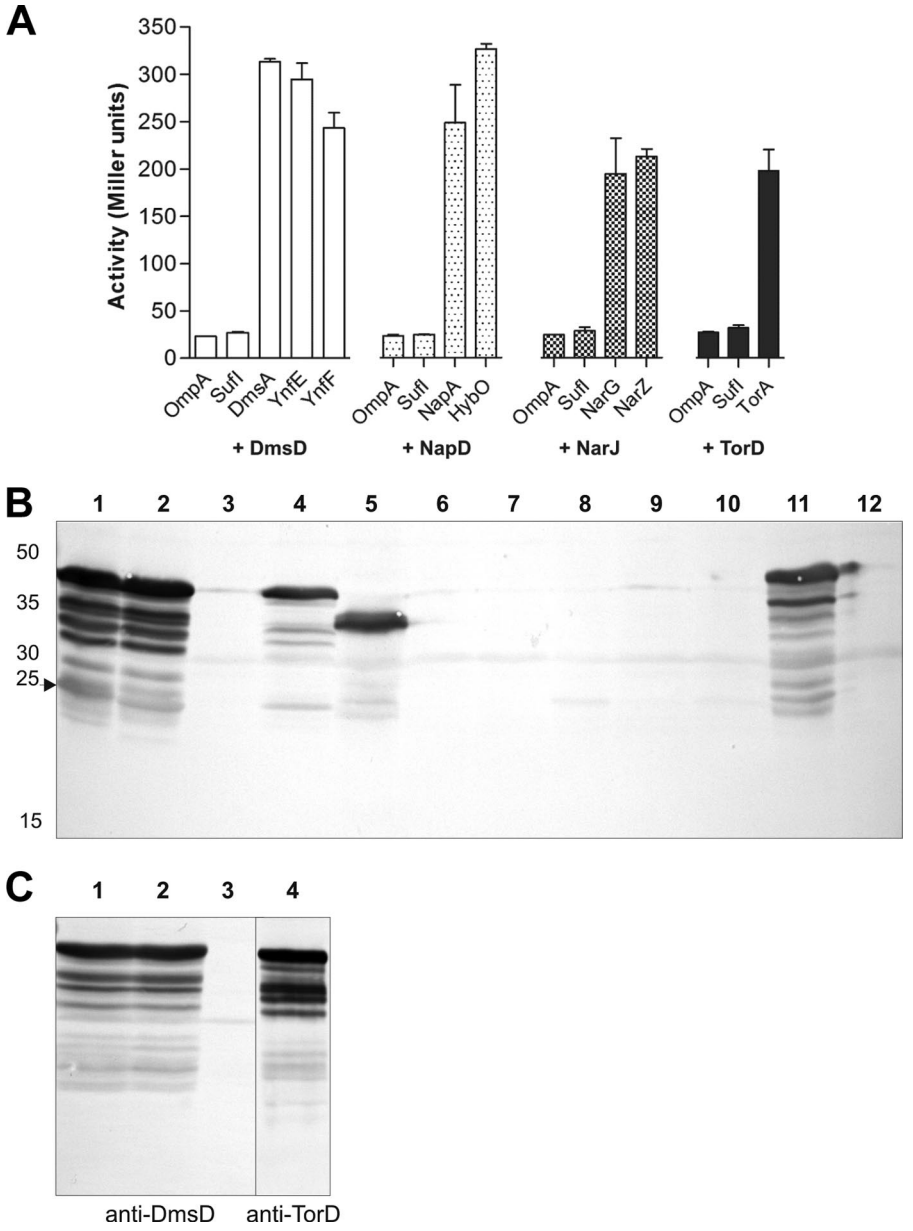

FIG. 3. BACTH studies of interactions between REMPs and RR peptides. (A) Assay of β-galactosidase activity as a reporter for the interaction between the REMP-T25 and RR peptide-T18 fusions. All 170 interaction pairs were tested, but only those showing activity above that of the negative controls, OmpA and SufI, are plotted here. Bars indicate standard errors. (B) Western blot of cultures coexpressing both REMP and RR peptide fusions, using an anti-CyaA antibody against the T25 and T18 portions of adenylate cyclase. Lanes: 1, DmsD/DmsA; 2, DmsD/YnfE; 3, DmsD/TorA; 4, TorD/TorA; 5, NapD/NapA; 6, NapD/HybO; 7, HyaE/HyaA; 8, HybE/HybO; 9, HybE/OmpA; 10, HybE/SufI; 11, NarJ/NarG, 12, YcdY/BisZ. The arrowhead indicates accumulation of the DmsA leader. (C) Western blot of the samples from panel B but probed with anti-DmsD or anti-TorD serum; only lanes 1 to 4 are shown.

noted that the high level of β-galactosidase activity from colonies was consistently observed only after the 30-day mark. Activities for interaction pairs that were near the basal level (i.e., activity of the OmpA and SufI controls) were omitted from Fig. 3A for simplicity. The addition of 0.1 mM IPTG to the plates or liquid culture medium to induce higher expression of the fusions for both assays did not alter the results (not shown).

The BACTH experiments confirmed those done similarly with NapD and the NapA leader peptide by another group (16). However, there is over a 20-fold difference in the magnitude of β-galactosidase activity in terms of Miller units. This is due to the nonstandardized protocol in assaying β-galactosidase activities from variations in culture growth and assay conditions. It has been recognized in an article reviewing the uses of *lacZ* for yeast two-hybrid studies that the assays are more useful when comparing results from internal controls (such as the OmpA and SufI leaders used here) that were treated identically during individual experiments (28).

The REMP/RR peptide interaction protects both from proteolytic degradation in vivo. False-negative results from protein expression and accumulation during the BACTH experiments were investigated via Western blots. Cell extracts carrying plasmids expressing the REMP and RR peptide BACTH constructs were tested for accumulation using a polyclonal antibody against adenylate cyclase. The results show that the combination pairs where the REMP and RR peptide do not interact via BACTH also did not accumulate (Fig. 3B shows a sample blot of various combinations). These are DmsD with TorA peptide (Fig. 3B, lane 3), HyaE with HyaA peptide (lane 7), HybE with HybO peptide (lane 8), and YcdY with BisZ peptide (lane 12). The same accumulation problem was also observed for HybE with the negative controls OmpA and SufI peptides (lanes 9 and 10, respectively). The ladder of bands for proteins that did accumulate (Fig. 3B, lanes 1, 2, 4, and 11) suggests that the protein fusions are highly protease sensitive in the cell, but they also point toward the possibility that an interaction between the REMPs and peptides may protect both from complete degradation. Western blots of the same samples were probed with anti-DmsD or anti-TorD sera and showed that the fragments correspond to DmsD or TorD (Fig. 3C), indicating that these are proteolytic fragments of the two. Accumulation of the DmsA leader was indicated by a much darker band corresponding to the theoretical size of DmsA leader-T18 present in the anti-CyaA blot (Fig. 3B).

Western blots against the REMP and peptide BACTH constructs individually failed to detect accumulation of any of the constructs when expressed alone (results not shown), further supporting the hypothesis that the interaction between the REMPs and the RR peptides is required for stabilizing the proteins from degradation in the BACTH screen. These observations appear to be specific to the BTH101 (*cyaA*-deficient) strain required for the screen, as expression of the peptide-T18 constructs in other *E. coli* strains, including those with REMP deletions, resulted in accumulation (data not shown). TorD has been implicated in signal peptide protection for the TorA leader (7); the observations here suggest that protection appears to be toward both components, where the interaction prevents both from being proteolytically fragmented. Samples used for far-Western and SPR (see below) experiments show the ability of the REMPs and RR peptide fusions to accumulate in the absence of each other, pointing toward a protective role under in vivo conditions in a *cyaA*-deficient strain. The protective roles of the two may explain the variable observation of the NapD-HybO leader interaction, where the two are partners that interact infrequently but, once they find each other, are stabilized and interact very strongly.

Far-Western analyses of multiple fusion constructs. While we were able to detect an interaction between TorD and TorA leader only via the in vivo BACTH method, prior observations of the two interacting in vitro have been reported (8, 21). This led us to test various TorA leader fusions by far-Western analyses to explore issues due to the fusion tag itself. Five different constructs in addition to the SBP fusion were tested. We recognized that the peptide-T18 fusions would not accumulate alone based on the data in Fig. 3B; the TorA leader-T18 construct was included here as a negative control. Of the six TorA leader fusions tested, none of them appeared to show an interaction with purified TorD (Fig. 4A, top panel). While

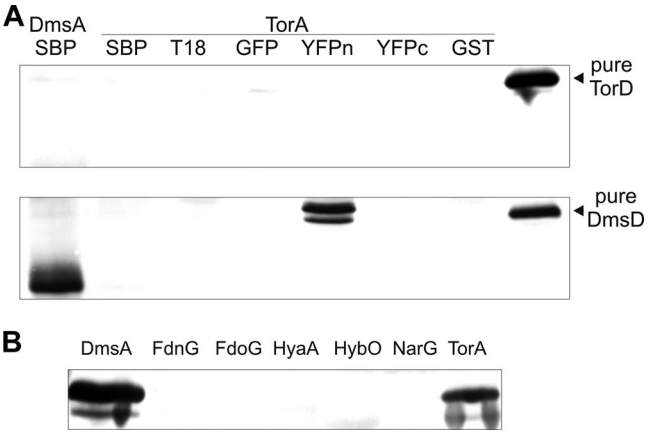

FIG. 4. Far-Western analyses of N-terminal/leader peptides with different fusion tags. (A) Far-Western blot against various TorA leader fusions. Blots were probed with 100 μg/ml of His_6-T_7-TorD (top) or His_6-T_7-DmsD (bottom), followed by 1:5,000 anti-T_7. (B) Far-Western blot against various RR peptides with the YFPn fusion. All 10 REMPs were tested, but only the DmsD-probed blot is shown here; probing conditions were as described for panel A.

the lack of interaction was expected for the T18 construct due to the lack of accumulation, the accumulation of the other constructs was confirmed using Western blotting against SBP, GFP, YFPn, YFPc, and GST, thus ruling out false-negative results. Interestingly, when these TorA peptide fusions were probed with purified DmsD, an interaction with the TorA leader-YFPn fusion was observed (Fig. 4A, bottom panel). The observations here confirm that the interaction between DmsD and apo-TorA demonstrated by immunoprecipitation in prior studies is indeed toward the RR-containing leader region of TorA (20). The results from this experiment demonstrate that the type of fusion appears to have an effect on the ability of the REMP to interact with the RR peptide.

Since the YFPn fusion appeared to allow for the detection of interaction between DmsD and the TorA leader, we selected a few other RR peptides to see if this fusion would allow for the detection of additional interactions. The peptides tested included DmsA, FdnG, FdoG, HyaA, HybO, NarG, and TorA. We were still unable to detect any extra interactions using these constructs, except that of DmsD toward TorA peptide as already confirmed above (Fig. 4B). Interestingly we were unable to detect any interaction between NarJ and NarG peptide-YFPn (results not shown) even though this interaction was observed by all the methods described above.

Biacore SPR analysis of interactions. A second in vitro approach via Biacore SPR was used to investigate the interaction between the REMPs and RR-containing peptides. In this experiment, the ligand (SBP-tagged RR peptides) is immobilized onto the surface of a sensor chip, followed by passage of the analyte (His-tagged REMPs) over the flow cell containing the RR peptides. A change in the density of material at the surface of the sensor chip alters the refractive index of the surface, corresponding to changes measured in resonance units. Due to the higher cost associated with these experiments, only N-terminal/leader peptides showing an interaction by the previous methods were screened against all of the REMPs. The leaders of BisZ, FdnG, and HybO were also

TABLE 3. Kinetic data for the REMPs and RR peptides showing an interaction by Biacore SPR analysis[a]

REMP and kinetic parameter	Value (mean ± SE)[b] with:					
	DmsA	NapA	NarG	NarZ	TorA	YnfE
DmsD						
K_D (nM)	**64 ± 3**	ND	ND	ND	ND	678 ± 47
k_a ($M^{-1} \cdot ms^{-1}$)	**31,400 ± 309**	ND	ND	ND	ND	188,000 ± 9,590
k_D (ms^{-1})	**2.0 ± 0.9**	ND	ND	ND	ND	127 ± 6
NapD						ND
K_D	ND	64 ± 11	ND	ND	ND	ND
k_a	ND	46,000 ± 1,730	ND	ND	ND	ND
k_D	ND	2.9 ± 0.5	ND	ND	ND	ND
NarJ						
K_D	ND	ND	**409 ± 46**	334 ± 19	ND	ND
k_a	ND	ND	**7,220 ± 371**	8,490 ± 158	ND	ND
k_D	ND	ND	**3.0 ± 0.3**	2.8 ± 0.2	ND	ND
NarW						
K_D	ND	ND	5,870 ± 309	**641 ± 34**	ND	ND
k_a	ND	ND	1,000 ± 45	**5,750 ± 125**	ND	ND
k_D	ND	ND	5.9 ± 0.2	**3.7 ± 0.2**	ND	ND
TorD						
K_D	ND	ND	ND	ND	3,760 ± 112	ND
k_a	ND	ND	ND	ND	3,050 ± 67	ND
k_D	ND	ND	ND	ND	12 ± 0.2	ND

[a] Each N-terminal RR peptide was tested against all 10 REMPs, but only ones showing an interaction are listed here. The peptides of BisZ, FdnG, HybO, and the OmpA control were also tested against all REMPs but are not shown due to the lack of any detectable interaction.
[b] When multiple partners exist, the cognate/predicted RR peptide is in bold. ND, no detectable interaction.

chosen along with the control of OmpA leader to rule out any technique-related problems that may have occurred with the above techniques. SPR confirmed most of the interactions observed by far-Westerns and BACTH, with the exception of the DmsD/TorA leader and NapD/HybO leader interactions. Additionally, an interaction between NarW and the N-terminal peptides of NarG and NarZ was observed (Table 3). An interesting observation from this experiment was that no FdnG-SBP protein was able to be immobilized on the surface of the chip, as seen by the lack of any discernible change in the sensorgram. This again supports the previous observations that we were unable to obtain accumulation of this construct under any growth and induction conditions.

The SPR experiments also allowed for the quantitation of the kinetics of the interaction through the on rate (k_a) and off rate (k_d) and of the strength of the interaction by calculating the equilibrium dissociation constant (K_D) from the kinetics. To calculate K_D, the following equation was used, based on a 1:1 Langmiur model of simple binding: $K_D = k_d/k_a$. For the REMPs that showed multiple binding partners via SPR, DmsD and NarW appeared to bind their expected RR peptide approximately 10-fold tighter, based on the calculated K_D values (Table 3). NarJ appeared to bind its expected substrate NarG at levels similar to those for NarZ, suggesting that although this REMP is specific for nitrate reductase RR-containing peptides, it does not appear to have a preference between the two. When the kinetics of the interactions was assessed, DmsD binding to YnfE leader had faster on and off rates than that to DmsA leader (Table 3). The rest of the interaction pairs had relatively slow on and off rates compared to those of DmsD binding to YnfE leader.

Secondary interaction sites determined by BACTH analysis. In recognition that secondary interaction sites in the mature region (i.e., the sequence following the N-terminal peptides) for the TorD/TorA (8) and NarJ/NarG (30) pairs have been previously observed, we investigated whether such sites existed in all the RR-containing redox enzymes in this study. Using the BACTH method described earlier, full-length proteins of each were fused to the T18 portion of adenylate cyclase as described above and analyzed for interactions with the REMPs. Assays by both colony observation and β-galactosidase activity showed similar interactions as with the peptides. Unlike in the peptide studies, interactions with the full-length forms of FdnG and FdoG with FdhE and of HybO with HybE were observed (Fig. 5). In comparisons of those that bound both the RR peptide and full protein, DmsD showed stronger interactions with the leader peptides than with the full protein, whereas NapD, NarJ, and TorD showed relatively similar interactions with both (Fig. 5). It should also be noted that the TorD/TorA and NarJ/NarZ pairs displayed fully red colonies in this screen, while their peptide counterparts displayed red colonies with white centers.

DISCUSSION

The vast selection of methods to study protein-protein interactions can be overwhelming when one is deciding on the appropriate method for a protein(s) of interest. Once the decision between in vitro versus in vivo techniques is made, there are still numerous options within both categories. This study explores the interactions between RR motif-containing peptides of Tat-dependent redox enzymes and their system-spe-

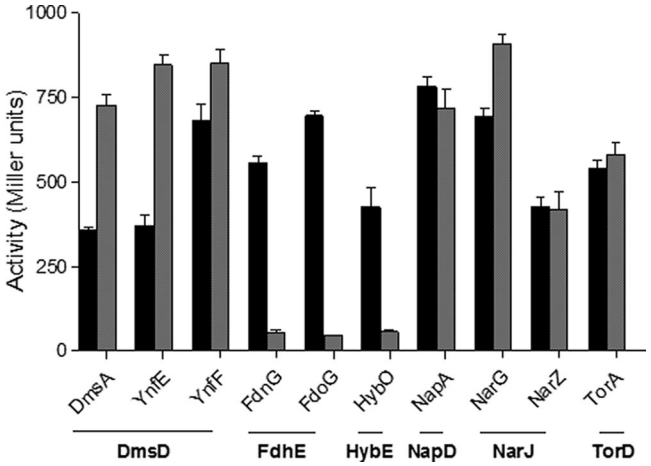

FIG. 5. Comparison of β-galactosidase activities of the REMPs with either the RR peptide (gray) or full-length RR proteins (black) obtained by BACTH assays. Full-length proteins include the RR peptide plus the mature region following the peptide sequence. Bars indicate standard errors.

cific chaperones, REMPs. Using a combination of in vitro and in vivo methods, interactions were identified and characterized based on the strength of interactions and their degree of specificity. The results are summarized in Table 4.

A total of 11 interactions between the REMP/RR peptide pairs were identified using a combination of various techniques. The difference in the methods that identified the interactions highlights the importance of the nature of the peptide display from its fusion tag both in vivo and in vitro. Unique interactions identified by one method are the DmsD/TorA leader, NapD/HybO leader, NarW/NarG peptide, and NarW/NarZ peptide pairs. Several interactions identified in this study are novel, while some confirm results previously obtained by our group and others. We also provide a systematic comparison of all known and predicted REMPs/RR peptides of the Tat system in this study. Despite our efforts, the interaction between HyaE and full-length HyaA and HybO demonstrated by Dubini and Sargent (6) was not detected by any of our methods. This is likely explained by their use of a different version of BACTH through λcI/RNA polymerase activation (6).

The in vivo BACTH method offered an alternative method to identify interactions, as this method allows for the potential influence of cellular factors. The BACTH screens confirmed most of the interactions observed by use of far-Western analysis and SPR (Table 4). Identification of additional interactions using full-length RR proteins suggests either that the binding site for FdhE and HybE is located in the mature region of the protein or that the preprotein form allows the leader peptide to be displayed in a folded conformation required for recognition by the REMPs. These results are not surprising, as direct interactions with the mature region (i.e., sequence following the RR leader peptide) have previously been observed for NarJ with NarG (30) and TorD with TorA (13). Using this screen, DmsD was the only REMP to show a significant difference in interaction activity (as measured by BACTH reporter activity) between the full-length protein and the leader peptides of DmsA, YnfE, and YnfF. If secondary sites in the mature region of the protein exist, one would expect the activity to be higher due to more cAMP activation of *lacZ*. However, if DmsD is a more efficient REMP in maturation and/or targeting of these substrates to the translocon, a lower activity would result as the "lifetime" of the apo-DmsA/DmsD interaction would be shorter, resulting in lower β-galactosidase activity. This is because the full-length protein constructs used contain the signal peptidase cleavage site that was excluded in the peptide constructs, meaning that their leaders can be processed. The differences between DmsD, TorD, and NarJ in terms of peptide promiscuity and apoenzyme processing suggest that while they belong to the same family of proteins based on sequence homology (29), each may be specifically required for slightly different maturation pathways of individual RR redox enzymes.

Using the kinetic data from Biacore SPR, we were able to obtain K_Ds for many of the interaction pairs (Table 3). In comparing all the K_D values obtained by SPR, we can rank the strength of the interactions based on their expected primary substrate as DmsD/NapD > NarJ > NarW ≫ TorD. Several K_Ds for the REMPs and RR peptides have been obtained by isothermal titration calorimetry by other groups: 223 nM for DmsD with a DmsA leader-GST fusion (31), 1,700 nM for TorD with a synthetic peptide of the TorA leader corresponding to residues 10 to 36 (10), 7 nM for NapD with a MalE-

TABLE 4. REMP substrate interactions identified in this study

REMP	Method(s)[a] identifying interaction with:							
	DmsA	HybO	NapA[b]	NarG	NarZ[b]	TorA	YnfE[b]	YnfF[b,c]
DmsD	fW_S, fW_Y, B_C, B_L, SPR	×	×	×	×	fW_Y	fW_S, B_C, B_L, SPR	fW_S, B_C, B_L
NapD	×	B_L	fW_S, B_C, B_L, SPR	×	×	×	×	×
NarJ	×	×	×	fW_S, B_C, B_L, SPR	fW_S, B_C, B_L, SPR	×	×	×
NarW	×	×	×	SPR	SPR	×	×	×
TorD	×	×	×	×	×	B_C, B_L, SPR	×	×

[a] fW_S, far-Western analysis with SBP fusion; fW_Y, far-Western analysis with YFPn fusion; B_C, BACTH red/white colony analysis; B_L, BACTH liquid culture analysis; SPR, Biacore SPR analysis (only RR peptides of BisZ, DmsA, FdnG, HybO, NapA, NarG, NarZ, TorA, and YnfE were tested against all REMPs by SPR). The lack of interaction between all other REMPs and RR peptides used in this study is either not shown in the table or indicated by ×.

[b] Far-Western analysis with the YFPn fusion was not tested.

[c] The YnfF leader should interact with DmsD under Biacore SPR analysis due to the strength of interaction observed with the other methods, but this was not tested in this study.

TABLE 5. Homology among RR peptide sequences

RR peptide	% Sequence identity/similarity with[a]:														
	BisC	BisZ	DmsA	FdnG	FdoG	HyaA	HybO	NapA	NarG	NarZ	TorA	YedY	YfhG	YnfE	YnfF
BisC	100/100	5/10	12/24	3/3	6/14	5/8	15/18	5/11	10/13	9/13	7/10	20/27	2/6	16/26	13/25
BisZ		100/100	21/35	33/49	36/52	23/37	16/32	38/51	1/3	1/3	22/31	20/31	10/13	20/35	23/37
DmsA			100/100	26/37	28/40	20/32	17/31	21/41	1/2	1/3	**22/36**	25/52	4/5	**37/54**	**57/81**
FdnG				100/100	**87**[b]**/87**	27/39	23/35	29/38	13/18	13/18	28/38	19/30	2/6	**29/41**	**19/26**
FdoG					100/100	25/36	23/35	43/53	12/17	8/8	32/39	17/23	1/3	29/38	23/37
HyaA						100/100	26/45	**21**[c]**/41**	6/14	4/14	29/45	19/30	12/20	22/42	25/46
HybO							100/100	**32/37**	3/3	3/3	23/35	13/27	12/17	30/44	20/31
NapA								100/100	3/6	3/6	21/30	23/32	11/22	28/49	24/45
NarG									100/100	**86/94**	15/18	0/8	1/1	7/15	1/1
NarZ										100/100	8/18	7/11	1/1	9/13	1/3
TorA											100/100	17/26	26/36	**27/39**	**19/27**
YedY												100/100	5/8	27/39	16/51
YfhG													100/100	1/4	2/2
YnfE														100/100	40/60
YnfF															100/100

[a] Values for pairs sharing common interaction partners are in bold. Alignments were done using EMBOSS pairwise alignment algorithms (22).

[b] Although an interaction between FdhE and FdnG/FdoG was observed only when the full-length RR-containing proteins were used, it is possible that the full-length protein causes the leader to adapt a confirmation required for recognition. Therefore, these two are considered to have common interactions to determine recognition specificity.

[c] An interaction between NapD and the HybO leader was observed, and HybE is the known REMP for HybO. However, according to Dubini and Sargent (6), HyaE also interacts with the HybO leader, and thus NapD and HyaE are concluded to have common RR peptide partners here.

NapA leader-His_6 sandwich fusion (16), and 164 nM for NarJ with a synthetic peptide of the first 50 residues of NarG (4). Our data allow for direct comparison, as all RR peptides were displayed in the same fashion. The TorD/TorA leader pair corresponds to the second weakest interaction from SPR data, which may explain why we were unable to detect this interaction in any of the far-Western experiments. However, since we were able to detect this interaction via the in vitro method of SPR but not via far-Western analysis, this also suggests that the interaction requires some sort of conformational freedom in solution that could be inhibited by a static conformation when sitting on the surface of a membrane. The NarW/NarG peptide pair was the weakest among all detected interactions, yet NarW bound its predicted substrate NarZ peptide approximately 10-fold tighter. This difference was also observed for DmsD with its expected substrate DmsA leader, suggesting a trend that the REMPs bind their expected substrate with ~10-fold-higher affinity when multiple substrates exist. The differences in interaction strengths with the RR peptide suggest that clues to specificity may also lie within the sequence of the mature portions of the proteins or at least in how the mature portion displays the leader sequence, as suggested by the BACTH data using full proteins.

The observation of cross-interaction partners for some of the REMPs could explain why studies involving REMP deletions resulted in properly targeted yet only partially functional redox enzymes, suggesting that the maturation pathways are similar but not exactly overlapping. A study involving a hybrid where the DmsA leader was replaced by the TorA leader sequence in DmsA resulted in properly targeted DMSO reductase but with greatly reduced cellular enzyme activity (24). While we demonstrate that DmsD interacts with the TorA leader peptide, it is more likely that this hybrid was targeted by TorD, since the DmsD/TorA leader interaction is observed only under very select conditions. Similar studies by Jack et al. showed that a hybrid with the HybO leader replacing the TorA leader sequence in TorA has lowered TMAO reductase activity that can be restored to that of the wild type by overexpressing TorD from a plasmid (13). A final indication of cross-reactivity of REMPs is demonstrated in a recent study where wild-type TorA or a TorA mutant impaired in TorD binding expressed in a Δ*torD* mutant is still localized to the periplasm with active, albeit reduced, TMAO reductase activity (3), again suggesting that another REMP (possibly DmsD) was responsible for targeting TorA to the membrane. Together these observations suggest that the cross-binding activities of REMPs could be useful under circumstances where a particular REMP is unavailable or changes in final electron acceptor availability force the cell to rapidly produce one type of redox enzyme. Since all three examples resulted in properly targeted enzymes with reduced activities, it appears that their recognition promiscuities can fully substitute for targeting, while the other steps of enzyme maturation still rely heavily on the cognate REMP.

The resulting interactions, summarized in Table 4, provide clues to the specificity of some REMPs of the Tat system. To better understand these observations and look for clues from homology, sequence alignments among the RR peptides and REMPs are shown in Tables 5 and 6, respectively. The RR peptides were also split into the RR motif and the hydrophobic region following the motif for separate alignments (see Table S2 in the supplemental material) due to previous observations that both of these elements in the TorA leader were required for tight association with TorD (10). Comparison of pairs sharing common interaction partners with other pairs indicates that homology of neither the REMPs nor RR peptides alone is sufficient to explain the observation of common interactions. The identity and similarity values for REMPs mostly support that homology is required for interaction with common RR peptides, with the exception of four REMP pairs (Table 6). The three exceptions involving YcdY are not surprising, as no RR peptide was found to interact with it in this study nor does

TABLE 6. Homology among REMP sequences

REMP	% Sequence identity/similarity with[a]:									
	DmsD	FdhD	FdhE	HyaE	HybE	NapD	NarJ	NarW	TorD	YcdY
DmsD	100/100	0.6/0.8	8/15	8/12	17/23	7/12	14/23	16/24	**19/30**	27/42
FdhD		100/100	11/18	10/15	13/19	4/6	21/34	5/8	13/24	7/13
FdhE			100/100	7/13	11/20	7/9	13/22	10/20	5/10	6/11
HyaE				100/100	12/19	**20**[b]**/28**	10/17	15/22	13/23	9/14
HybE					100/100	**9/18**	4/7	3/5	9/14	13/21
NapD						100/100	3/6	8/13	5/9	16/25
NarJ							100/100	**56/71**	18/27	14/25
NarW								100/100	19/28	18/30
TorD									100/100	20/34
YcdY										100/100

[a] Values for pairs sharing common interaction partners are in bold. Values equal to or greater than the lowest observed for common REMP pairs in a given set are underlined (in Table 5, RR peptides were excluded due to the large number of values in this category). Alignments were done using EMBOSS pairwise alignment algorithms (22).

[b] See Table 5, footnote *c*.

it have any known substrates or function to date, despite being part of the family that includes DmsD, NarJ, and TorD (29). The higher percent sequence identity and similarity of DmsD/HybE than for the observed NapD/HybE pairs suggest that homology of the REMPs is not the sole factor determining whether two REMPs will interact with the same RR peptide.

While alignment of the entire RR peptide did not fully explain the observation of common REMP interactions by functionally unrelated enzymes, comparison of the motif and hydrophobic region alignments indicates that the RR motif does not correlate to REMP recognition specificity (see Table S2 in the supplemental material). This is expected, as the motif is known for Tat-specific recognition and targeting of substrates. The hydrophobic region offers some explanation but is not as clear as with the REMPs, as many peptide pairs have higher homology than those with common interactions. When focusing on those with common interactors, alignments of the hydrophobic region identify a common pattern with a short continuous string of small, hydrophobic residues located 2 to 10 residues after the RR motif (Fig. 1B). Comparison of the DmsD and NapD interactors suggests that the length of this stretch of residues correlates to binding specificity, as the DmsD/TorA leader and NapD/HybO leader interactions were observed under selective conditions and their hydrophobic stretch varied the most from the expected substrates of the DmsA and NapA leaders, respectively. The inability to define a definitive REMP-specific binding motif suggests that the key identification residues of the leader have not been fully delineated. Interestingly, V23 of the hydrophobic stretch in the TorA leader was one of five residues identified for TorD binding in a recent study involving glutamine-scanning mutagenesis of the TorA leader (3). The remaining four residues (L27, G28, L31, and L32) reside after the continuous stretch described here, with L31 being the only residue that is identical within all DmsD interactors based on the alignment (Fig. 1B). Perhaps these residues confer specificity to TorD, a REMP that is not as promiscuous as DmsD.

The sequence alignments provide some conclusions with regard to the mechanism of substrate specificity by the REMPs. Homology of both the entire REMP sequences and the hydrophobic regions of RR peptides confers recognition specificity, with emphasis on the position and length of the continuous hydrophobic stretch following the RR motif. The varying architecture of this hydrophobic stretch is likely to adapt to the binding pockets of different REMP structural classes such as those recently described by Maillard et al. (16). The findings presented here provide insight into the chaperone selectivity of redox enzymes that utilize the Tat system.

This study thoroughly investigated the ability of the known REMP chaperones in *E. coli* to interact with RR motif-containing peptides from their respective redox enzymes. Our study demonstrates that each REMP is indeed a system-specific chaperone and that the display of the leader is critical for identification and interaction to occur. The results further suggest that each redox enzyme system that incorporates an RR-like leader follows a different maturation pathway requiring its own chaperone to facilitate its unique pathway toward a folded, targeted, assembled, and functional enzyme.

ACKNOWLEDGMENTS

This work was supported by a Canadian Institute of Health Research grant to R.J.T. C.S.C. is funded by a PGS-D scholarship from the Natural Sciences and Engineering Research Council of Canada. Funding for the Biacore instrument was from the Canadian Foundation of Innovation "Cybercell" initiative.

We thank Jenika Howell for construction of recombinant NapD, NarJ, NarW, TorD, and YcdY used in this study. The anti-DmsD and anti-TorD sera were gifts from Frank Sargent. We also thank Aaron Yamniuk for assistance with the Biacore instrument.

REFERENCES

1. **Bendtsen, J. D., H. Nielsen, G. von Heijne, and S. Brunak.** 2004. Improved prediction of signal peptides: SignalP 3.0. J. Mol. Biol. **340:**783–795.
2. **Berks, B. C.** 1996. A common export pathway for proteins binding complex redox cofactors? Mol. Microbiol. **22:**393–404.
3. **Buchanan, G., J. Maillard, S. B. Nabuurs, D. J. Richardson, T. Palmer, and F. Sargent.** 2008. Features of a twin-arginine signal peptide required for recognition by a Tat proofreading chaperone. FEBS Lett. **582:**3979–3984.
4. **Chan, C. S., J. M. Howell, M. L. Workentine, and R. J. Turner.** 2006. Twin-arginine translocase may have a role in the chaperone function of NarJ from *Escherichia coli*. Biochem. Biophys. Res. Commun. **343:**244–251.
5. **Chenna, R., H. Sugawara, T. Koike, R. Lopez, T. J. Gibson, D. G. Higgins, and J. D. Thompson.** 2003. Multiple sequence alignment with the Clustal series of programs. Nucleic Acids Res. **31:**3497–3500.
6. **Dubini, A., and F. Sargent.** 2003. Assembly of Tat-dependent [NiFe] hydrogenases: identification of precursor-binding accessory proteins. FEBS Lett. **549:**141–146.
7. **Genest, O., F. Seduk, M. Ilbert, V. Mejean, and C. Iobbi-Nivol.** 2006. Signal peptide protection by specific chaperone. Biochem. Biophys. Res. Commun. **339:**991–995.

8. **Genest, O., M. Neumann, F. Seduk, W. Stocklein, V. Mejean, S. Leimkuhler, and C. Iobbi-Nivol.** 2008. Dedicated metallochaperone connects apoenzyme and molybdenum cofactor biosynthesis components. J. Biol. Chem. **283:** 21433–21440.
9. **Hanahan, D.** 1983. Studies on transformation of *Escherichia coli* with plasmids. J. Mol. Biol. **166:**557–580.
10. **Hatzixanthis, K., T. A. Clarke, A. Oubrie, D. J. Richardson, R. J. Turner, and F. Sargent.** 2005. Signal peptide-chaperone interactions on the twin-arginine protein transport pathway. Proc. Natl. Acad. Sci. USA **102:**8460–8465.
11. **Howell, J. M., and R. J. Turner.** 2004. The role of redox enzyme maturation proteins (REMPs) in the biogenesis of *Escherichia coli* oxidoreductases: the example of DMSO reductase. Recent Res. Dev. Microbiol. **8:**1–14.
12. **Ilbert, M., V. Mejean, and C. Iobbi-Nivol.** 2004. Functional and structural analysis of members of the TorD family, a large chaperone family dedicated to molybdoproteins. Microbiology **150:**935–943.
13. **Jack, R. L., G. Buchanan, A. Dubini, K. Hatzixanthis, T. Palmer, and F. Sargent.** 2004. Coordinating assembly and export of complex bacterial proteins. EMBO J. **23:**3962–3972.
14. **Karimova, G., A. Ullmann, and D. Ladant.** 2001. Protein-protein interaction between *Bacillus stearothermophilus* tyrosyl-tRNA synthetase subdomains revealed by a bacterial two-hybrid system. J. Mol. Microbiol. Biotechnol. **3:**73–82.
15. **Karimova, G., N. Dautin, and D. Ladant.** 2005. Interaction network among *Escherichia coli* membrane proteins involved in cell division as revealed by bacterial two-hybrid analysis. J. Bacteriol. **187:**2233–2243.
16. **Maillard, J., C. A. E. M. Spronk, G. Buchanan, V. Lyall, D. J. Richardson, T. Palmer, G. W. Vuister, and F. Sargent.** 2007. Structural diversity in twin-arginine signal peptide-binding proteins. Proc. Natl. Acad. Sci. USA **104:**15641–15646.
17. **Miller, J. H.** 1972. Molecular cloning: a laboratory manual. Cold Spring Harbor, New York, NY.
18. **Miroux, B., and J. E. Walker.** 1996. Over-production of proteins in *Escherichia coli*: mutant hosts that allow synthesis of some membrane proteins and globular proteins at high levels. J. Mol. Biol. **260:**289–298.
19. **Natale, P., T. Brüser, and A. J. M. Driessen.** 2008. Sec- and Tat-mediated protein secretion across the bacterial cytoplasmic membrane—distinct translocases and mechanisms. Biochim. Biophys. Acta **1778:**1735–1756.
20. **Oresnik, I. J., C. L. Ladner, and R. J. Turner.** 2001. Identification of a twin-arginine leader-binding protein. Mol. Microbiol. **40:**323–331.
21. **Pommier, J., V. Mejean, G. Giordano, and C. Iobbi-Nivol.** 1998. TorD, a cytoplasmic chaperone that interacts with the unfolded trimethylamine N-oxide reductase enzyme (TorA) in *Escherichia coli*. J. Biol. Chem. **273:** 16615–16620.
22. **Rice, P., I. Longden, and A. Bleasby.** 2000. EMBOSS: The European Molecular Biology Open Software Suite. Trends Genet. **16:**276–277.
23. **Richardson, D. J.** 2000. Bacterial respiration: a flexible process for a changing environment. Microbiology **146:**551–571.
24. **Sambasivarao, D., R. J. Turner, J. L. Simala-Grant, G. Shaw, J. Hu, and J. H. Weiner.** 2000. Multiple roles for the twin arginine leader sequence of dimethyl sulfoxide reductase of *Escherichia coli*. J. Biol. Chem. **275:**22526–22531.
25. **Santini, C.-L., A. Bernadac, M. Zhang, A. Chanal, B. Ize, C. Blanco, and L.-F. Wu.** 2001. Translocation of jellyfish green fluorescent protein via the Tat system of *Escherichia coli* and change of its periplasmic localization in response to osmotic up-shock. J. Biol. Chem. **276:**8159–8164.
26. **Sarfo, K. J., T. L. Winstone, A. L. Papish, J. M. Howell, H. Kadir, H. J. Vogel, and R. J. Turner.** 2004. Folding forms of *Escherichia coli* DmsD, a twin-arginine leader binding protein. Biochem. Biophys. Res. Commun. **315:** 397–403.
27. **Sargent, F.** 2007. Constructing the wonders of the bacterial world: biosynthesis of complex enzymes. Microbiology **153:**633–651.
28. **Serebriiskii, I. G., and E. A. Golemis.** 2000. Uses of *lacZ* to study gene function: evaluation of β-galactosidase assays employed in the yeast two-hybrid system. Anal. Biochem. **285:**1–15.
29. **Turner, R. J., A. L. Papish, and F. Sargent.** 2004. Sequence analysis of bacterial redox enzyme maturation proteins (REMPs). Can. J. Microbiol. **50:**225–238.
30. **Vergnes, A., J. Pommier, R. Toci, F. Blasco, G. Giordano, and A. Magalon.** 2006. NarJ chaperone binds on two distinct sites of the aponitrate reductase of *Escherichia coli* to coordinate molybdenum cofactor insertion and assembly. J. Biol. Chem. **281:**2170–2176.
31. **Winstone, T. L., M. L. Workentine, K. J. Sarfo, A. J. Binding, B. D. Haslam, and R. J. Turner.** 2006. Physical nature of signal peptide binding to DmsD. Arch. Biochem. Biophys. **455:**89–97.